ARTICLES

Hydrated Electron Yields in the Heavy Ion Radiolysis of Water

Jay A. LaVerne,*,†,‡ Igor Štefanić,† and Simon M. Pimblott†,‡

Radiation Laboratory and Department of Physics, University of Notre Dame, Notre Dame, Indiana 46556

Received: June 7, 200; In Final Form: August 22, 2005

Experimental measurements coupled with Monte Carlo track simulations have been used to examine the yields of hydrated electrons in the radiolysis of water with protons, helium ions, and carbon ions. Glycylglycine, in concentrations ranging from 10^{-4} to 1 M, was employed as a scavenger and the production of the ammonium cation used as a probe of hydrated electron yields from about 2 ns to 20 μs. Monte Carlo track simulations employing diffusion-kinetic calculations of product yields are found to reproduce experimental observations satisfactorily. Model details are used to elucidate the heavy ion track physics and chemistry. Comparison of the heavy ion results with those found in γ radiolysis shows intratrack reactions are significant on the nanosecond to microsecond time scale as the ion track relaxes, and that a constant (escape) yield is never attained on this time scale. Numerical interpolation techniques are used to obtain both track average and track segment yields for use in practical applications or comparison with other models. The model results give the first hints that initial (∼5 ps) hydrated electron yields, and possibly other water decomposition products, are dependent on the type and energy of the incident radiation.

Introduction

The hydrated electron is the principal reducing species produced in the radiolysis of water, and yet very little information exists on its yield or kinetics in the tracks of heavy ions. Most of our knowledge on the hydrated electron has been accumulated using pulsed electron radiolysis techniques employing optical detection.[1,2] Protons, helium ions, and other heavy ions have a larger linear energy transfer rate (LET = the stopping power, $-dE/dx$) than fast electrons. Heavy ion tracks in water are characterized by regions of high energy-deposition density and thereby higher concentrations of water decomposition products than are found with γ-rays or fast electrons.[3] Second-order reactions are enhanced in heavy ions tracks leading to a decrease in hydrated electron yields. For example, studies have shown that hydrated electron yields at about 1 μs following the passage of the ionizing radiation decrease with increasing energy deposition density within the heavy ion track from a value of about 2.5 electrons/100 eV with γ-rays to 0.25 electrons/100 eV with low-energy helium ions.[1,3] Little is known about the relative kinetics leading to this decrease, since the only direct measurements of the hydrated electron decay with heavy ions have been performed with protons or with ions of very high energy.[4−8] Knowledge on the temporal dependence of the hydrated electron yield is valuable for comparison with model predictions that give a detailed description of the track structure. The decay kinetics of the hydrated electron is also important in a number of technological applications, including nuclear power production and radioactive waste management.

The yield of the hydrated electron with heavy ions has been determined directly from its absorption in three cases. Burns and co-workers measured the decay of the hydrated electron in a water jet irradiated with 3 MeV protons.[4−6] The absorbance of the hydrated electron was found to have a greater rate of decay with 3 MeV protons in the time range of 1 to 30 ns than that observed with fast electrons. Extrapolation of the data to shorter times gave yields consistent with the concept that the initial yield for the formation of the hydrated electron is the same for all types of radiation. The LET of 3 MeV protons is not very high (12 eV/nm) and the local density of radiation-induced species in the track is only slightly greater than that with fast electrons (0.2 eV/nm). Consequently, little information on ion tracks of higher density can be inferred from these studies. Sauer et al. determined the yield of the hydrated electron as a function of penetration depth for 20 MeV deuterons and 40 MeV helium ions by observing the absorbance of the electron in a segment of the ion track.[9,10] These experiments do not give the time decay of the hydrated electron, but rather the yields following ion beam pulses of ∼10 μs width. Substantial decay of the hydrated electron occurs within the duration of the pulse, complicating data analysis. The data show that the yield of the hydrated electron decreases by about an order of magnitude with a variation in LET from 5 to 50 eV/nm, and that the yield with helium ions is greater than that with deuterons of the same LET. Baldacchino et al. observed the decay of the hydrated electron absorption following pulses of 1.1 GeV ^{12}C, 1.5 GeV ^{16}O, and 3.4 GeV ^{36}Ar ions.[7,8] The absolute yields inferred seem to be somewhat higher than expected from the other studies. All of these results are useful for drawing general conclusions about the ion track structure. Elucidation of track processes would be greatly facilitated by more information on the yield of the hydrated electron at shorter times and over a wider range of heavy ion energies and LET.

Heavy-ion pulse-radiolysis experiments are very difficult to perform, so the majority of information on the yields of hydrated electrons has been determined by using solutes as selective

† Radiation Laboratory.
‡ Department of Physics.

10.1021/jp0530303 CCC: $30.25
Published on Web 10/01/2005

hydrated electron scavengers.[11−16] The stable product formed in a scavenging experiment can be used as a quantitative measurement of the hydrated electron yield. Several different scavenging systems have been developed for the hydrated electron, including chloroacetic acid, nitrous oxide, nitrate, and glycylglycine. The scavenging capacity of these scavenger systems is equivalent to the product of the solute concentration and the rate coefficient for the scavenging reaction, i.e., the pseudo-first-order rate coefficient with unit of s^{-1}. The inverse of the scavenging capacity gives a measure of the lifetime of the hydrated electron with respect to the scavenging reaction. For most of the experiments previously used to study hydrated electron yields, the scavenging capacity of the solute employed corresponds to about 1 μs. This time scale is relatively long in the evolution of the heavy ion track. Knowledge about the kinetics of the hydrated electron can be derived from the variation in product yield as a function of the scavenging capacity, which is obtained by changing solute concentration. The considerable advantage of this technique is that it effectively allows one to probe the kinetics of the hydrated electron by measuring stable product yields. Only one study of the kinetics of the hydrated electron for heavy ion radiolysis has been made with use of scavengers. Yoshida and LaVerne examined the helium ion radiolysis of glycylglycine solutions, equating the yield of the hydrated electron with the formation of the ammonium cation from the scavenging reaction of glycylglycine.[15] In this study, the previous experiments of Yoshida and LaVerne are repeated, using a more accurate analytic technique for product analysis. Glycylglycine solutions are also irradiated with other heavy ions to obtain a more complete set of hydrated electron kinetics, and to systematically examine the effects on ion track structure on the radiation chemistry of the hydrated electron over a wide variety of ion types and energies.

This work presents the yield of the hydrated electron as determined by the formation of ammonium cation by the scavenging reaction of glycylglycine. Irradiations were made with protons of energy 2 to 15 MeV, helium ions of energy 5 to 20 MeV, and carbon ions of 10 to 30 MeV initial energy. The temporal dependence of the hydrated electron was determined over the time scale of about 2 ns to 20 μs by variation of the glycylglycine concentration from 10^{-4} to 1 M. Track segment yields are derived from the energy dependence of the measured track average yields. The experimental data are compared with predictions from Monte Carlo track simulations that include the track structure, the nonhomogeneous chemical kinetics, and the diffusion of the reactive radiation-induced species. These comparisons provide an understanding of the physical track structure from the scavenger yields. The effect of track structure on the yields and kinetics of the hydrated electron for different energy heavy ion irradiations is discussed.

Experimental Section

The irradiations were performed at the FN Tandem Van de Graaff facility of the University of Notre Dame Nuclear Structure Laboratory. The window assembly and irradiation procedure were the same as reported earlier.[17,18] Completely stripped ^{1}H, ^{4}He, and ^{12}C ions were used with total beam currents of about 1 nA (charge current = ion current times ion charge, Z). Heavy ion energy was determined to within 0.1% by magnetic analysis, and the energy loss to windows was determined from standard stopping power tables.[19] Absolute dosimetry was performed by collecting and integrating the charge from the sample cell and exit window in combination with the ion energy. Total doses were 3.2×10^{19} eV in 20 mL of solution (250 Gy). All ions were stopped completely in the sample, so track-averaged yields were measured.

The samples were irradiated in a Pyrex sample cell with a thin mica window ($\sim$6 mg/cm^2) attached. The sample cell contained a magnetic stirrer that was operated continuously during the radiolysis. Oxygen was purged from the solution throughout the irradiation by bubbling with argon or helium. Glycylglycine (Sigma Chemical Company) was recrystallized[20] and dissolved in water purified by an in-house H2Only commercial system, consisting of a UV lamp and various micoporous filters. The solutions were irradiated at their natural pH (5.4−5.7) and were transferred to sample vials for analysis. The yield of ammonium ions produced by the reaction of the hydrated electron with glycylglycine was measured within a few hours of the radiolysis with use of a Dionex DX 500 ion chromatographic system. The ion chromatograph was calibrated with standard ammonium chloride solutions. The estimated accuracy of the ammonium cation determination is ±5%.

Monte Carlo track simulations were performed using the same general techniques and parameters as in previous studies.[21] There are three components to each calculation: (i) simulation of a realistic track structure for the transfer of energy from the ionizing radiation to the medium, (ii) determination of the physical consequences of each energy transfer event, i.e., ionization or electronic or vibrational excitation, and (iii) kinetic modeling of the competition between the relaxation of the spatially nonhomogeneous distribution of radiation-induced reactants and their reactions either within the track or with scavengers.

The track structure methodology uses a collision-by-collision approach employing liquid-phase inelastic collision cross-sections derived following the formalism of Ashley[22] and of Green and co-workers,[23] and using experimental gas-phase vibrational and elastic collision cross-sections.[21] The effects of charge cycling on the inelastic collision cross-section are incorporated by using experimentally determined gas-phase cross-sections for protons, and employing an effective charge correction for ^{4}He and ^{12}C ions. The use of the gas-phase cross sections for elastic collisions and charge cycling processes does not introduce significant errors as shown by the accuracy of heavy ion track simulations in predicting yields of the Fricke dosimeter.[21] Each track structure simulation determines the relative positions of all the energy loss events along the heavy ion track and for all the secondary electrons ejected. The physicochemical processes, i.e., water fragmentation, are determined from the energy loss in a collision event by using experimentally based probabilities for liquid and gaseous water, and the spatial placement of the water fragmentation products is relative to the parent energy-loss event. Diffusion-reaction kinetics of the radiation-induced reactive species is modeled by using the independent reaction times (IRT) methodology, which is based upon the independent pairs approximation that is implicit in the Smoluchowski−Noyes treatment of diffusion-limited reaction.[24] The chemistry of $\sim 10^3$ different tracks is modeled to obtain statistically meaningful kinetics. Typically, track segments of 10−100 keV attenuation are considered. A series of track segment yields are calculated at different ion energies, and are then integrated to give track average yields for the complete stopping of the heavy ion.[25]

Results and Discussion

Track Average or Integral Yields. Glycylglycine is used as a scavenger of the hydrated electron to estimate the hydrated

electrons yield at various times in the evolution of heavy ion tracks. Previous studies have shown that glycylglycine reacts with the hydrated electron to give the ammonium cation, which is measured in these experiments.[20]

$$^{+}NH_3CH_2CONHCH_2CO_2^{-} + e_{aq}^{-} + H_2O \rightarrow {}^{\bullet}CH_2CONHCH_2CO_2^{-} + NH_4^{+} + OH^{-}$$

The rate coefficient for this reaction is 3×10^8 M^{-1} s^{-1} and all indications are that the reaction is quantitative. Glycylglycine exists in aqueous solutions as a Zwitter ion and the hydrated electron is scavenged by the positively charged amine group. Cleavage to give ammonia is fast so further reactions of the anion adduct in heavy ion tracks are expected to be negligible. The extensive studies with γ radiolysis have shown that reactions of OH radicals and H atoms with glycylglycine do not lead to ammonia production.[20]

$$^{+}NH_3CH_2CONHCH_2CO_2^{-} + {}^{\bullet}OH \rightarrow {}^{+}NH_3CH_2CONH^{\bullet}CHCO_2^{-} + H_2O$$

$$^{+}NH_3CH_2CONHCH_2CO_2^{-} + {}^{\bullet}H \rightarrow {}^{+}NH_3CH_2CONH^{\bullet}CHCO_2^{-} + H_2$$

Glycylglycine concentrations employed were 10^{-4}, 10^{-3}, 10^{-2}, 10^{-1}, and 1 M and correspond to times of ca. 10^{-5}, 10^{-6}, 10^{-7}, 10^{-8}, and 10^{-9} s, respectively, in the evolution of the track chemistry.

The ranges of the heavy ions used in this work are short relative to the depth of the sample chamber. For instance, a 15 MeV proton has a range of 2.5 mm in water while that of a 10 MeV carbon ion is only 13 μm. Experimental yield measurements represent a track average for all ion energies from the incident energy to zero. Frequently, these yields are called integral track yields, because of the self-summation along the ion track. Integral yields are the most common type of yield experimentally measured with scavengers, but are difficult to relate to track structure directly because of the inherent averaging over a range of energy, LET, and other ion characteristics.

The effect of initial ion energy, E_o, on the production of the ammonium cation (G_oE_o, molecules/100 incident ions) is shown in Figures 1−3 for protons, helium ions, and carbon ions, respectively. Each figure contains the results over four decades of glycylglycine concentration from 0.1 mM to 1 M. The amount of ammonium cation formed increases super-linearly with increasing ion energy. At a given ion energy, the amount of ammonium cation formed decreases with decreasing glycylglycine concentration reflecting the relative reduction in the hydrated electron yield with time, to be discussed in more detail below. Direct absorption spectroscopy, material balance, and model calculations suggest that the limiting short-time yield of the hydrated electron is ∼4.2 electron/100 eV for γ-rays and fast electron pulse radiolysis.[25−27] The maximum ammonium cation production (that would be measured at "infinite" glycylglycine concentration) should correspond to this yield. This asymptotic yield is given by the solid lines in the three figures. Comparison of the experimental data to this limiting yield shows the effect of increasing LET. Increasing the reactant density within the radiation track leads to a readily observed decrease in the amount of ammonium cation formed for a given glycylglycine concentration from protons to helium ions to carbon ions.

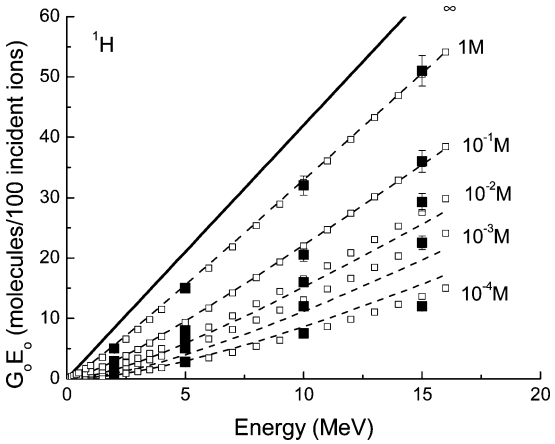

Figure 1. Production of ammonium cation ($G_oE_o(NH_4^+)$, molecules/100 incident ions) as a function of initial proton energy, E_o, for glycylglycine concentrations of 10^{-4}, 10^{-3}, 10^{-2}, 10^{-1}, and 1 M. The open symbols are a fit to the data with use of eq 1 and the dashed lines are predictions from Monte Carlo track simulations. The solid line is the expected amount of ammonium cation production for infinite solute concentration and corresponds to an initial yield of 4.2 hydrated electrons/100 eV.

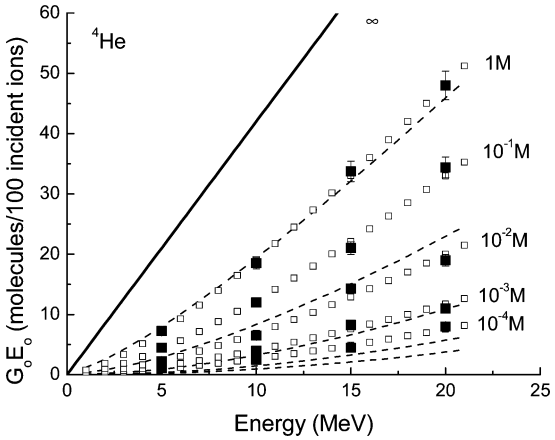

Figure 2. Production of ammonium cation ($G_oE_o(NH_4^+)$, molecules/100 incident ions) as a function of initial helium ion energy, E_o, for glycylglycine concentrations of 10^{-4}, 10^{-3}, 10^{-2}, 10^{-1}, and 1 M. The open symbols are a fit to the data with use of eq 1 and the dashed lines are predictions from Monte Carlo track simulations. The solid line is the expected amount of ammonium cation production for infinite solute concentration and corresponds to an initial yield of 4.2 hydrated electrons/100 eV.

Radiation chemical yields are conventionally presented in terms of the *G*-value, with the unit of molecules/100 eV of total energy absorption. Integral heavy ion yields at a particular ion energy are obtained by dividing the amount of ammonium cation produced, G_oE_o, by the incident ion energy, E_o. Consequently, in Figures 1−3 an integral yield is the slope of a line from the origin to the datum at the initial ion energy of interest. Integral yields for each of the experimental measurements are shown in Figures 4−6 for protons, helium ions, and carbon ions, respectively. To interpolate to different ion energies and to determine track segment yields, the measured integral yields were fit to an analytic function developed in previous work on the Fricke dosimeter.[28] The production of ammonium cation, G_oE_o, at incident ion energy, E_o, is assumed to have the form,

$$G_oE_o = G_BE_o + (G_\infty - G_B)(E_o - E_B)F \qquad (1)$$

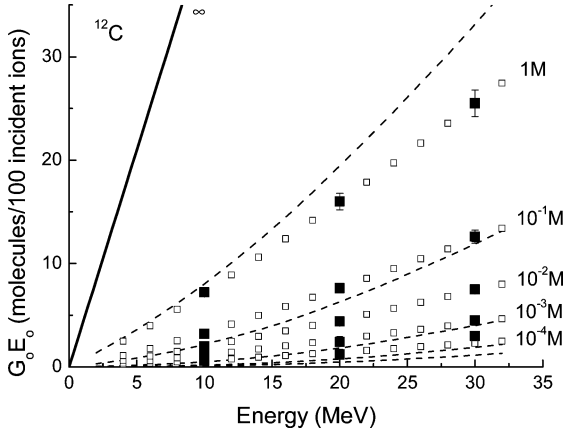

Figure 3. Production of ammonium cation ($G_oE_o(NH_4^+)$, molecules/100 incident ions) as a function of initial carbon ion energy, E_o, for glycylglycine concentrations of 10^{-4}, 10^{-3}, 10^{-2}, 10^{-1}, and 1 M. The open symbols are a fit to the data with use of eq 1 and the dashed lines are predictions from Monte Carlo track simulations. The solid line is the expected amount of ammonium cation production for infinite solute concentration and corresponds to an initial yield of 4.2 hydrated electrons/100 eV.

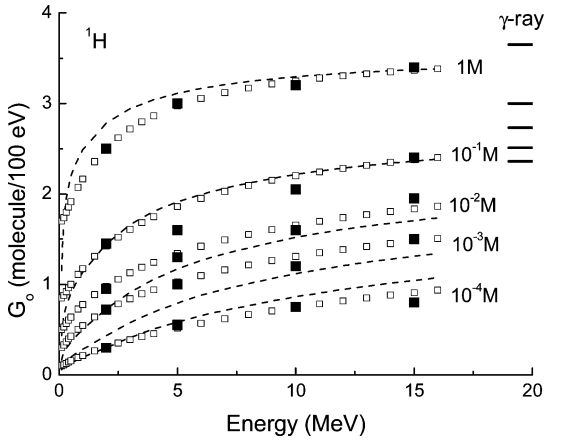

Figure 4. Track averaged yields (G_o, molecules/100 eV) as a function of initial proton energy, E_o, for glycylglycine concentrations of 10^{-4}, 10^{-3}, 10^{-2}, 10^{-1}, and 1 M. The open symbols are from eq 2, using the same fitting parameters as in Figure 1, and the dashed lines are predictions from Monte Carlo track simulations. The limiting yield for each glycylglycine concentration observed with γ-rays is also shown, ref 20.

where F is a dimensionless factor given by

$$F = a(E_o - E_B)^m/(1 + a(E_o - E_B)^m) \qquad (1a)$$

with G_B being the yield at the energy, E_B, corresponding to the Bragg peak, and a and m being fitted parameters. The incorporation of the parameters representing the Bragg peak is necessary since the LET goes through a maximum at this point and experimental determination of yields below this energy is extremely difficult due to straggling and other effects. A linear response, G_BE_o, is assumed below the Bragg peak. Only a small fraction of the measured product is formed below the Bragg peak at the energies of the ions examined here so the assumption of a linear response in this region is expected to be reasonable. The value of G_∞ corresponds to the high-energy limit (given by γ-rays) at the same glycylglycine concentration. The open symbols in Figures 1−3 show the fits to the experimental integral yields with use of eqs 1 and 1a. A different set of parameters is obtained for each ion at each glycylglycine concentration. In all cases, the fits faithfully reproduce the experimentally measured values.

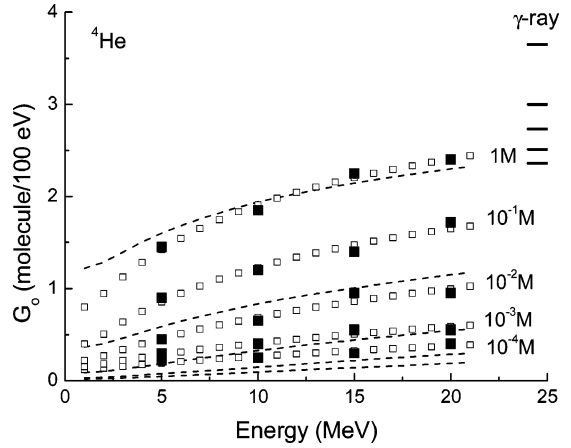

Figure 5. Track averaged yields (G_o, molecules/100 eV) as a function of initial helium ion energy, E_o, for glycylglycine concentrations of 10^{-4}, 10^{-3}, 10^{-2}, 10^{-1}, and 1 M. The open symbols are from eq 2, using the same fitting parameters as in Figure 2, and the dashed lines are predictions from Monte Carlo track simulations. The limiting yield for each glycylglycine concentration observed with γ-rays is also shown, ref 20.

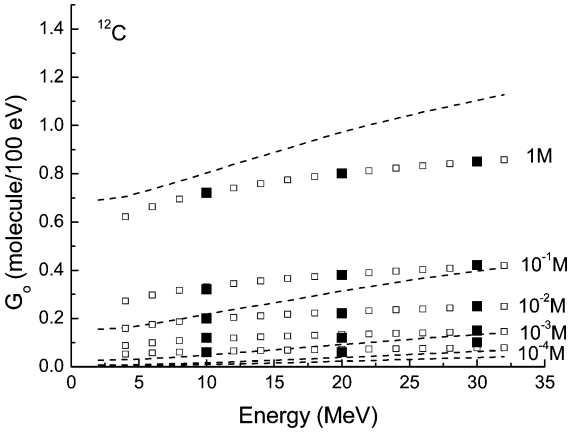

Figure 6. Track averaged yields (G_o, molecules/100 eV) as a function of initial carbon ion energy, E_o, for glycylglycine concentrations of 10^{-4}, 10^{-3}, 10^{-2}, 10^{-1}, and 1 M. The open symbols are from eq 2, using the same fitting parameters as in Figure 3, and the dashed lines are predictions from Monte Carlo track simulations. The limiting yield for each glycylglycine concentration observed with γ-rays is also shown, ref 20.

An interpolation formula for integral track yields can be obtained by a simple rearrangement of eq 1 to give

$$G_o = G_B + (G_\infty - G_B)(1 - E_B/E_o)\,F \qquad (2)$$

where the parameters are the same as above. The fitting of eqs 1 and 1a to the data in Figures 1−3 leads to a self-consistent set of integral (and differential) yields and simplifies interpolation to different ion energies. The energy-dependent integral yields predicted by the empirical equations are given in Figures 4−6 as open symbols.

The Monte Carlo track simulations explicitly consider only small sections of a radiation track in which heavy ion characteristics such as energy and LET remain essentially constant. Computer limitations on the number of reactive species modeled at one time restrict the examination of the entire ion track chemistry to low heavy ion energies or to track segments. Comparison of model predictions with experimentally determined track average yields requires the summation of a series of segments for different ion energies. The integral yields predicted by Monte Carlo track simulations are shown as the

dashed lines in Figures 1−6. The agreement between experiment and simulation is best for protons and gets progressively poorer for helium ions and then carbon ions. This disagreement is not surprising given the increased uncertainty in the simulation model for ions with increased mass and nuclear charge. Experimental collision cross-sections for inelastic, elastic, and charge-cycling processes have been more extensively examined for protons. The Bragg peak for protons in water occurs at $\sim 10^5$ eV, so the track-end represents only a small portion of the attenuation of a 2 MeV ion—the lowest energy studied. The density of radiation-induced reactants in proton tracks in water is not sufficiently high to cause concern about the breakdown of the independent pairs approximation, which is the basis of the independent reaction times methodology. Breakdown of the independent pairs approximation will occur when the concentration of reactants is sufficiently high that interreactant forces (e.g. Coulombic) modify the chemistry. This effect was not observed in modeling the radiolysis of the Fricke dosimeter with Ni ions.[21] In contrast, the collision cross-sections employed in the simulation of the tracks of heavier ions are less certain, and the effects of charge cycling are incorporated by using an effective nuclear charge. Furthermore, as the LET of the radiation particle increases and the density of track reactants increases, breakdown of the independent pairs approximation is possible. Considering the wide range of track geometries for this range of ions, the agreement between experiment and simulation is reasonable. The largest differences between predicted yields and experiment are observed at the lowest glycylglycine concentrations, which correspond to the longest times in the track evolution. The origins of this discrepancy may lie in both sets of data. The ammonium cation yields are very low for 0.1 and 1 mM glycylglycine solutions and are difficult to measure accurately. The component of the track structure probed at the long time limit is the tail of the spatial distribution for the thermalization/solvation of the hydrated electron. The track structure simulations employed here assume a Gaussian spatial distribution of standard deviation ~5 nm. This distribution was derived by fitting the decay kinetics of the hydrated electron from fast electron pulse radiolysis.[21] Recently, Monte Carlo simulations of the attenuation of low-energy electrons in amorphous water have suggested a distribution with the same mean width, but different profile.[29] This profile has a very different tail extending to longer distances, which would suggest different long-time kinetics. All product distributions will tend to be Gaussian at long times because of diffusion, but one developing from an initially non-Gaussian distribution with a wide tail will have a different width at long times, with different kinetics, than an initially Gaussian distribution with the same mean.

The integral yields increase with increasing heavy ion energy because of the decreased density of radiation-induced species in the track with decreasing LET. At the same energy, the integral yields decrease from protons to helium ions to carbon ions because of increasing LET and track density. Increasing the concentration of reactive water products leads to an enhancement in second-order reactions giving reduced radical yields, including that of the hydrated electron, hydroxyl radical, and hydrogen atom. The complementary effect is an increase in the yields of molecular hydrogen, hydrogen peroxide, and water reformation. At the highest energy, heavy ion tracks should give results comparable to that of γ-rays because of the similarity in track structures.[3] Each of the limiting ammonium cation yields for the various glycylglycine concentrations are shown as the solid lines in Figures 4−6. For protons and helium ions at the highest glycylglycine concentrations, the yields will approach that for γ-rays at energies not much greater than those used in the present studies. The local spatial distributions of reactants within the spurs of high-energy protons and γ-ray tracks will be similar, but the separation between the spurs comprising the proton track will be smaller than that of the γ-ray because of its higher LET. Eventually the spurs of the proton's track will overlap giving slightly different product yields at longer times than observed for γ-rays.

Track Segment or Differential Yields. Track segment or differential yields, G_i, describe the chemistry within a track segment in which heavy ion characteristics such as energy and LET remain essentially constant. While this quantity is directly calculated by the Monte Carlo simulations, it must be derived from the experimental integral track yields. In theory, with sufficient experimental data at small energy intervals, track segment yields can be determined directly from the experimental measurements. However, this approach is not practical. A track segment yield at a given energy is equal to the tangent to the data of Figures 1−3. Instead of measuring a large number of data at different energies, track segment yields are obtained from the data of Figures 1−3, using the fitting discussed earlier and taking the derivative of the empirical eq 1 to give the following.

$$G_i = G_B + (G_\infty - G_B)[(1+m)a(E_o - E_B)^m + (a(E_o - E_B)^m)^2]/(1 + a(E_o - E_B)^m)^2 \quad (3)$$

Track segment yields can be obtained for each of the sets of data by using the previously determined fitting parameters. The outcome is not presented for the sake of brevity, but the trends in the track segment yields as a function of energy are the same as those for the track average yields. The agreement between track segment yields predicted by Monte Carlo track simulations and measured experimentally is comparable to that observed for the track average yields, i.e., the best agreement is for protons and the biggest discrepancies are for helium and carbon ions at low glycylglycine concentrations. Track segment and track average yields approach the same value when the ion energy approaches zero and when the yield becomes independent of energy at very high energies. Ammonium cation yields for 0.1 and 1 M glycylglycine solutions found with γ-rays are very similar to the track segment yields for protons of energy above 15 MeV. This agreement suggests that the higher energy track segments of the latter resemble a string of spurs rather than a continuous track.

Track segment yields are often presented as a function of LET to show the relative dependence of yields on track density. Track segment yields given by eq 3 are presented in Figure 7 as a function of the track segment LET for each of the ions at three glycylglycine concentrations. Also shown are the limiting yields with γ-rays. The figure shows a decrease in ammonium cation yields with increasing LET due to enhanced second-order reaction with increasing density of reactants in the track segment. The results also reveal that the track segment yield is not uniquely determined by LET. Several studies have shown that LET is not an adequate parameter to characterize yields in the heavy ion radiolysis of water.[1,3,10,21] Heavy ions of different velocity can have the same LET, but there are significant differences in the microscopic track structure due to the spatial distributions of the ejected secondary electrons. Previous Monte Carlo track simulations on the Fricke dosimeter suggested that the parameter MZ^2/E is a better indicator than LET for describing the long time yields in heavy ion radiolysis, where M, Z, and E are the mass, charge, and energy of the incident ion, respectively.[21] Figure 8 shows the track segment yields of ammonium

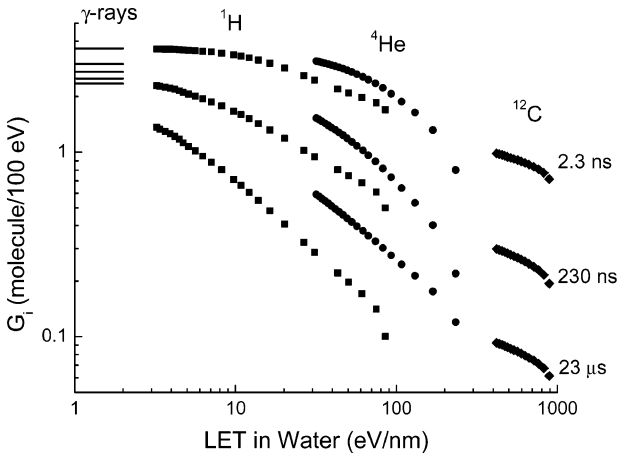

Figure 7. Track segment yields (G_i, molecules/100 eV) as a function of track segment LET (eV/nm) from eq 3, using the fitting parameters appropriate for (■) protons, (●) helium ions, and (◆) carbon ions at three glycylglycine concentrations corresponding to 2.3 ns, 230 ns, and 23 μs. The limiting yield for each glycylglycine concentration observed with γ-rays is also shown, ref 20.

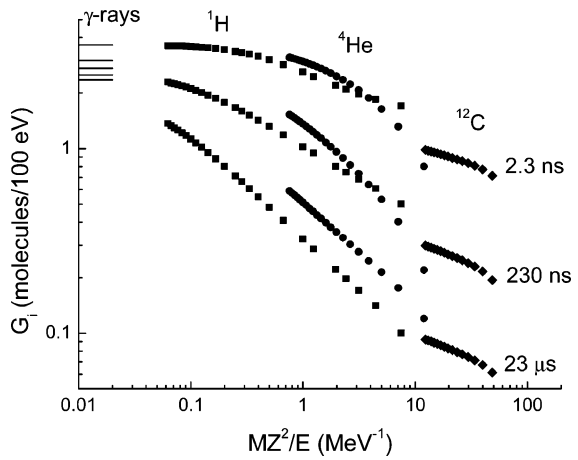

Figure 8. Track segment yields (G_i, molecules/100 eV) as a function of MZ^2/E (MeV^{-1}) from eq 3, using the fitting parameters appropriate for (■) protons, (●) helium ions, and (◆) carbon ions at three glycylglycine concentrations corresponding to 2.3 ns, 230 ns, and 23 μs. The limiting yield for each glycylglycine concentration observed with γ-rays is also shown, ref 20.

cation plotted as a function of MZ^2/E. An increase in the parameter MZ^2/E is similar to an increase in LET in that the density of species in the track becomes denser and radical yields decrease. The parameter MZ^2/E does not uniquely characterize the product yields for the different systems at all times, although it does provide a better parametrization than LET. Radical yields are not observed to change on the microsecond time scale in the radiolysis of water with fast electrons or γ-rays, because the isolated spurs have dissipated and the reactive species are well separated throughout the medium.[1−3] The rate of spatial relaxation of a heavy ion track and thereby the kinetics of the transient species depends on the velocity and the charge of the incident ion. The complexity of the effects of track structure makes it very difficult to predict yields at a particular time with different ions with use of a simple parametric fit appropriate to all systems. Such an approach may work for some systems such as the Fricke dosimeter, but is unlikely to be universally applicable.[21]

Scavenging Capacity and Time Dependences. Radicals produced in the decomposition of water are undergoing combination reactions in competition with the diffusive relaxation

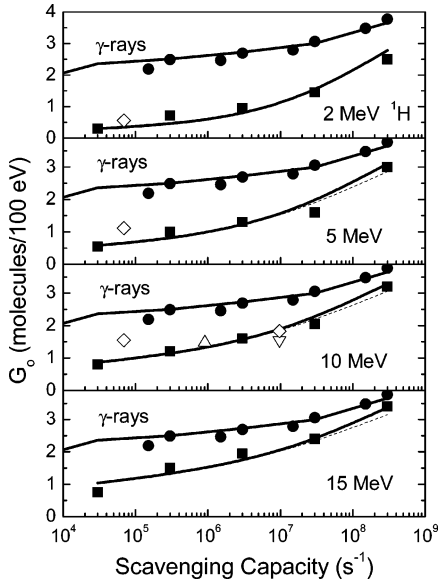

Figure 9. Scavenging capacity dependence of track average yields for protons of different energy. The solid lines are predictions from Monte Carlo track simulations and the data include (●) γ-rays, ref 20, (◇) 19.8, 10.0, and 4 MeV ^{2}H, refs 9 and 10, (△) 18 MeV ^{2}H, ref 12, and (▽) 23 MeV ^{2}H, ref 16. Deuteron data are plotted at half energy.

of the nonhomogeneous distribution of transients making up the heavy ion track. The reactions are second order in neat water and thereby dependent on the local concentrations of reactants. The addition of a solute introduces a competitive first-order reaction that can be used as a temporal probe of the amount of a given transient species assuming the product does not undergo subsequent intratrack chemistry. In this work, the scavenging of the hydrated electron by glycylglycine to produce the ammonium cation is taken to be representative of the hydrated electron yield. The scavenging capacity of the solute for radiation-induced reactants is given by the product of its concentration and the associated rate coefficient, which is equivalent to the pseudo-first-order rate coefficient. The inverse of the scavenging capacity is a measure of the lifetime of the hydrated electron with respect to the scavenging reaction. Comprehensive studies have shown that the inverse Laplace transform of the scavenging capacity dependence gives a reasonably accurate description of the time dependence of the transient species, even for heavy ion radiolysis.[30] Rarely does sufficient scavenging data exist for an accurate application of the inverse Laplace transform so other approximation methods are used. Studies on the temporal decay of hydroxyl radicals have shown that the half-life, i.e., ln(2)/scavenging capacity, is a good approximation for the conversion of scavenging data to the appropriate time scale of the decay kinetics.[31] In this work, the scavenging capacity dependence is used as a test of the accuracy of Monte Carlo track simulations. The simulations predict product yields directly for a given set of experimental conditions. The experimental measurements provide a stringent test of the ability of the methodology to correctly predict the radiation-chemical kinetics and to give a reasonable description of the underlying physical characteristics of the ion track.

The yields of ammonium cation produced in the radiolysis of glycylglycine solutions are shown in Figures 9−11 as a function of the scavenging capacity for proton, helium, and carbon ion radiolysis, respectively. The data of Appleby and Schwarz for 18 MeV deuterons (plotted at half energy) and for 12 MeV helium ions, shown in Figures 9 and 10, refer to the

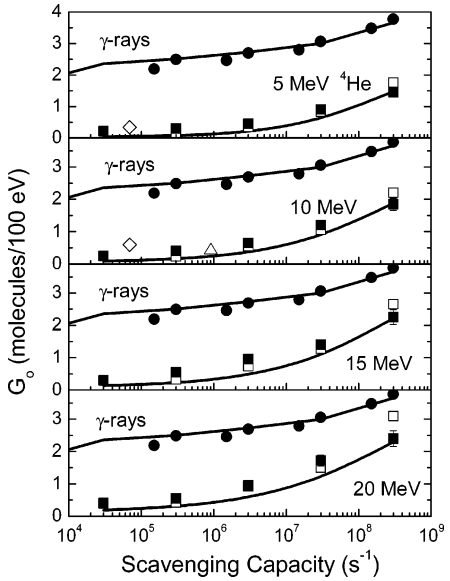

Figure 10. Scavenging capacity dependence of track average yields for helium ions of different energy. The solid lines are predictions from Monte Carlo track simulations and the data include (●) γ-rays, ref 20; (◇) 8.1 and 5.3 MeV ^{4}He, refs 9 and 10; (△) 12 MeV ^{4}He, ref 12; and (□) ^{4}He, ref 15.

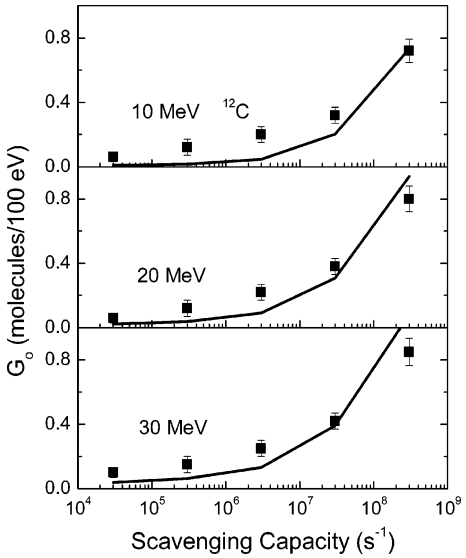

Figure 11. Scavenging capacity dependence of track average yields for carbon ions of different energy. The solid lines are predictions from Monte Carlo track simulations.

yield of nitrogen obtained with nitrous oxide as a hydrated electron scavenger.[12] Their results are in good agreement with the present work. Also shown in Figure 9 is the yield of nitrite measured for 23 MeV deuterons (plotted at half energy) with nitrate as a scavenger, which also agrees with the present results.[16] Sauer and co-workers used time-resolved methods to determine hydrated electron yields from the scavenging of perchlorate as measured at about 10 μs in pulsed deuteron and helium ion radiolysis.[9,10] Their data have been converted to a scavenging capacity dependence and the derived results in Figures 9 and 10 show good agreement with the present work. Glycylglycine was used as a scavenger of hydrated electrons in a previous study with helium ions.[15] That work used an ion selective electrode to measure the ammonia cation. Figure 10 shows that the largest deviations between the previous study and this work occur at the lowest glycylglycine concentration.

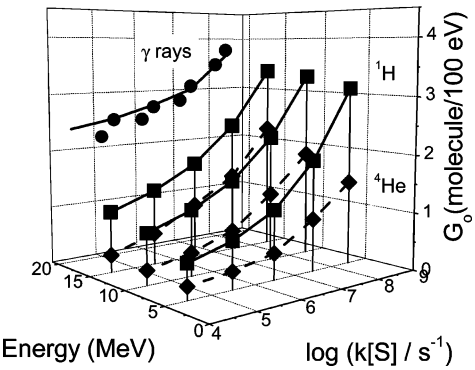

Figure 12. Track average yields of the hydrated electron as a function of energy and scavenging capacity for (■) protons and (◆) helium ions, this work, and (●) γ-rays, ref 20. The lines are from Monte Carlo track simulations.

The ion chromatographic technique is far superior to use of an ion selective electrode for accurately measuring small ammonium cation concentrations.

The data in Figures 9−11 show that a considerable amount of track chemistry occurs on the nanosecond to microsecond time scale. Furthermore, there is no "escape yield" as typically observed with fast electron or γ radiolysis. Heavy ion tracks have pseudo-two-dimensional symmetry and the track structure does not completely relax on the microsecond time scale. The predictions of the Monte Carlo track simulations are included in Figures 9−11 and are in reasonable agreement with the experimental results for all the heavy ions with the largest deviations occurring with carbon ions. Carbon ions undergo extensive charge exchange reactions as the ion slows down and an accurate prediction of the effective charge in liquid water is difficult.

A sense of the relative differences in the hydrated electron time dependences for protons and helium ions is revealed in Figure 12 where the yields are given as a function of both the heavy ion energy and the scavenging capacity. At large scavenging capacities, equivalent to short times, the yields for protons are very nearly the same as those with γ-rays. There is a steady decrease in yields with decreasing scavenging capacity, increasing time, and with decreasing heavy ion energy.

The power of an experiment-with-simulation approach to radiation chemistry is that predictions of yields can be made for conditions difficult to examine directly. The direct time measurement of hydrated electron decay in a standard pump/probe experiment is problematical with heavy ions because of their very short range. Burns and co-workers examined the transient decay of the hydrated electron in a jet of water irradiated with 3 MeV protons.[4−6] Their results are shown in Figure 13 with results from the Monte Carlo track simulations. The experiments used a water jet of about 0.15 mm, which is the range of a 3 MeV proton in water so track average yields were measured. Simulation predictions for both the track average and the track segment yields are shown in the figure. The track average decay kinetics agrees well with the experimental data. The largest deviation between calculation and experiment is found at the very longest times. Monte Carlo track simulations for 1 GeV ^{12}C ions in neat water accurately reproduce the time dependence of the experimental decay kinetics of Baldacchino et al.[8] However, the calculated absolute yields are smaller than the experimental values by a constant factor of ~40%. According to Baldacchino, the yield of the hydrated electron at 5 ns is about 4.7 electrons/100 eV, which is significantly larger than the accepted value of about 3.2 electrons/100 eV experimentally

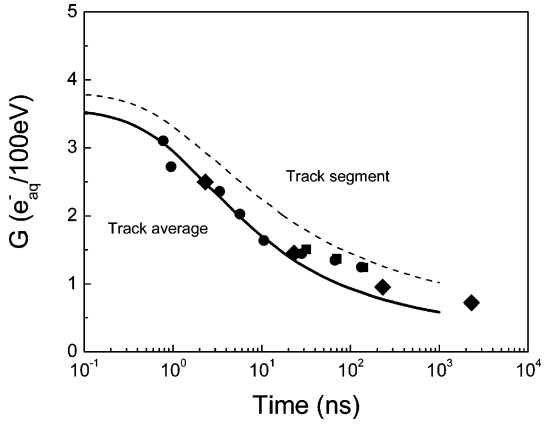

Figure 13. Measured time dependence of the hydrated electron decay with 3 MeV protons (■, ●, refs 4−6), the results of Monte Carlo track simulations for track average (solid line) and track segment (dashed line) yields, and (◆) scavenging capacity results for 2 MeV protons, this work.

TABLE 1: Yields of Ionization, Conduction Band Electrons, and Hydrated Electrons Produced in Radiolysis

	G(ionization)	$G(e_{cb}^-)$	$G(e_{aq}^-)$ at 5 ps
γ radiolysis	4.34	4.14	4.14
5 MeV H ion	4.32	3.89	3.88
5 MeV He ion	4.31	3.54	3.43
10 MeV C ion	4.30	2.95	2.60

measured in fast electron pulse radiolysis. The most obvious interpretation of this discrepancy is a significant error in dosimetry of the ^{12}C ion radiolysis experiments.

Effect of Track Structure on Initial Yields. A feature of the Monte Carlo track simulations is the ability to examine the physical track characteristics and the very short time radiation chemistry of heavy ions. These aspects of radiolysis are difficult to explore with other experimental and theoretical methods. Extrapolation of the experimental time decays of the hydrated electron for 3 MeV proton radiolysis to shorter times suggests that the initial yield of the hydrated electrons is similar to that for fast electron or γ-rays, i.e., ~4.2 molecules/100 eV. However, a 3 MeV proton has a relatively low LET (12 eV/nm) and the local density of radiation-induced species in the track is not much greater than that with fast electrons (0.2 eV/nm). The scavenger data dependences of Figure 9−11 suggest a considerably lower yield of hydrated electrons on the nanosecond time scale.

Most previous radiation chemical studies have assumed that the transient species in heavy ion tracks are formed with the same yield as in γ radiolysis and that intertrack radical reactions on the subnanosecond time scale are responsible for the decreased yields of hydrated electrons.[3] The Monte Carlo simulation methodology used in these studies explicitly contains the subpicosecond transformation of the electron from the conduction band and the intermediate energy "p" state to the ground "s" state, the hydrated electron. This decay is in competition with combination reactions of the electron with the water cation, H_2O^+, to form excited water molecules. Table 1 shows qualitative predictions from the Monte Carlo track simulations for the yields of ionization, conduction band electrons, and hydrated electrons produced with three heavy ions. The time-dependent kinetics is shown in Figure 14.

The early physicochemical processes were modeled in the simulations by assuming that ionization events lead to the

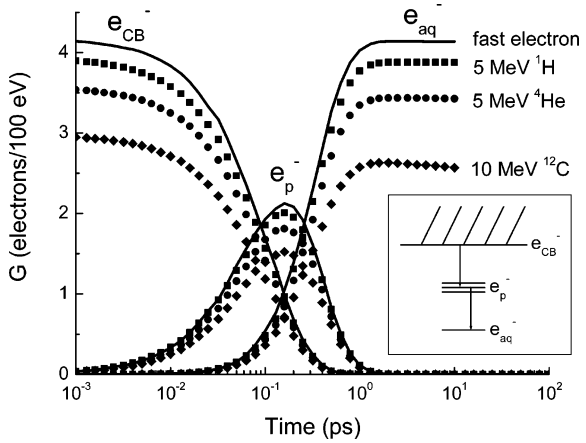

Figure 14. Time dependence of the conversion of conduction band electrons, e_{CB}^-, to "p" state electrons, e_p^-, to hydrated electrons, e_{aq}^-, from Monte Carlo track simulations for (■) 5 MeV protons, (●) 5 MeV helium ions, and (◆) 10 MeV carbon ions.

production of a water cation and, ultimately, a conduction band electron.

$$H_2O \rightarrow e_{cb}^- + H_2O^+$$

The water cation then reacts with adjacent solvent molecules

$$H_2O^+ + H_2O \rightarrow {}^{\bullet}OH + H_3O^+$$

producing a hydronium ion and the hydroxyl radical at times <100 fs. The conduction band electron undergoes relaxation, trapping, and hydration to produce the hydrated electron

$$e_{cb}^- \rightarrow \rightarrow \rightarrow e_{aq}^-$$

at times <300 fs. Alternatively, the two species may recombine in a geminate or random way

$$H_2O^+ + e_{cb}^- \rightarrow {}^{(1,3)}H_2O^*$$

to produce excited singlet or triplet states. The simulations consider this ultrafast process as a static reaction, using a cross section for the gas phase at thermal energy, k_BT,[32] which has been shown to reproduce the nonscavengable yield of H_2 in γ radiolysis.[21]

The effects of track structure are evident at even the earliest times. Measurements of W values suggest that the energy to form an ion pair is independent of the radiation type.[33] Therefore, the total ionization of water is expected to be independent of ion type and energy, which is found in the simulations as shown in Table 1. However, Figure 14 clearly suggests that many of the ion pairs are recombining on very fast time scales and there is a lower yield of hydrated electron with higher LET particles. These results are the first to suggest that the yields of initial water decomposition products are dependent on heavy ion type and energy. As previously noted, a decrease in the yields of hydrated electrons with increasing LET or track density is accompanied by an increase in the yield of molecular hydrogen.[1−3] Significant variation in the initial yields of all water radiolysis products with LET may be found in future studies.

Acknowledgment. We thank Professor A. Aprahamian for making the facilities of the Notre Dame Nuclear Structure Laboratory available. The latter is funded by the National Science Foundation. This contribution is NDRL-4610 from the

Notre Dame Radiation Laboratory, which is supported by the Office of Basic Energy Sciences of the U.S. Department of Energy.

References and Notes

(1) Allen, A. O. *The Radiation Chemistry of Water and Aqueous Solutions*; Van Nostrand: New York, 1961.

(2) Buxton, G. V. In *Charged Particle and Photon Interactions with Matter*; Mozumder, A., Hatano, Y., Eds.; Marcel Dekker: New York, 2004; Chapter 12.

(3) LaVerne, J. A. In *Charged Particle and Photon Interactions with Matter*; Mozumder, A., Hatano, Y., Eds.; Marcel Dekker: New York, 2004; Chapter 14.

(4) Burns, W. G.; May, R.; Buxton, G. V.; Tough, G. S. *J. Chem. Soc., Faraday Discuss.* **1977**, *63*, 47.

(5) Burns, W. G.; May, R.; Buxton, G. V.; Wilkinson-Tough, G. S. *J. Chem. Soc., Faraday Trans.* **1981**, *77*, 1543.

(6) Rice, S. A.; Playford, V. J.; Burns, W. G.; Buxton, G. V. *J. Phys. E* **1982**, *15*, 1240.

(7) Baldacchino, G.; Vigneron, G.; Renault, J. P.; Pin, S.; Remita, S.; Abedinzadeh, Z.; Deycard, S.; Balanzat, E.; Bouffard, S.; Gardes-Albert, M.; Hickel, B.; Mialocq, J. C. *Nucl. Instrum. Methods B* **2003**, *209*, 219.

(8) Baldacchino, G.; Vigneron, G.; Renault, J.-P.; Pin, S.; Abedinzaeh, Z.; Balanzat, E.; Bouffard, S.; Gardes-Albert, M.; Hickel, B.; Mialocq, J.-C. *Chem. Phys. Lett.* **2004**, *385*, 66.

(9) Sauer, M. C., Jr.; Schmidt, K. H.; Hart, E. J.; Naleway, C. A.; Jonah, C. D. *Radiat. Res.* **1977**, *70*, 91.

(10) Naleway, C. A.; Sauer, M. C. J.; Jonah, C. D.; Schmidt, K. H. *Radiat. Res.* **1979**, *77*, 47.

(11) Henglein, A.; Asmus, K.-D.; Scholes, G.; Simic, M. *Z. Phys. Chem.* **1965**, *45*, 39.

(12) Appleby, A.; Schwarz, H. A. *J. Phys. Chem.* **1969**, *73*, 1937.

(13) Yokohata, A.; Tsuda, S. *Bull. Chem. Soc. Jpn.* **1974**, *47*, 2869.

(14) Appleby, A.; Christman, E. A.; Jayko, M. *Radiat. Res.* **1986**, *106*, 300.

(15) LaVerne, J. A.; Yoshida, H. *J. Phys. Chem.* **1993**, *97*, 10720.

(16) Elliot, A. J.; Chenier, M. P.; Ouellette, D. C.; Koslowsky, V. T. *J. Phys. Chem.* **1996**, *100*, 9014.

(17) LaVerne, J. A.; Schuler, R. H. *J. Phys. Chem.* **1987**, *91*, 5770.

(18) LaVerne, J. A.; Schuler, R. H. *J. Phys. Chem.* **1987**, *91*, 6560.

(19) Ziegler, J. F.; Biersack, J. P.; Littmark, U. *The Stopping Power and Range of Ions in Solids*; Pergamon: New York, 1985.

(20) Yoshida, H.; Bolch, W. E.; Jacobson, K. B.; Turner, J. E. *Radiat. Res.* **1990**, *121*, 257.

(21) Pimblott, S. M.; LaVerne, J. A. *J. Phys. Chem. A* **2002**, *106*, 9420.

(22) Ashley, J. C. *J. Electron Spectrosc. Relat. Phenom.* **1988**, *46*, 199. Ashley, J. C. *J. Appl. Phys.* **1991**, *69*, 674.

(23) Green, N. J. B.; LaVerne, J. A.; Mozumder, A. *Radiat. Phys. Chem.* **1988**, *32*, 99.

(24) Rice, S. A. *Diffusion-limited Reactions*; Elsevier: Amsterdam, The Netherlands, 1985.

(25) Pimblott, S. M.; Mozumder, A. In *Charged Particle and Photon Interactions with Matter*: *Chemical, Physicochemical, and Biological Consequences with Applications*; Mozumder, A., Hatano, Y., Eds.; Marcell-Dekker Inc.: New York, 2004.

(26) Bartels, D. M.; Cook, A. R.; Mudaliar, M.; Jonah, C. D. *J. Phys. Chem. A* **2000**, *104*, 1686.

(27) Muroya, Y.; Lin, M.; Wu, G.; Iijima, H.; Yoshii, K.; Ueda, T.; Kudo, H.; Katsumura, Y. *Radiat. Phys. Chem.* **2005**, *72*, 169.

(28) LaVerne, J. A.; Schuler, R. H. *J. Phys. Chem.* **1994**, *98*, 4043.

(29) Green, N. J. B.; Pimblott, S. M. *Res. Chem. Intermed.* **2001**, *27*, 529 and related unpublished calculations.

(30) Pimblott, S. M.; LaVerne, J. A. *J. Phys. Chem.* **1992**, *96*, 746.

(31) LaVerne, J. A. *Radiat. Res.* **1989**, *118*, 201.

(32) Rosén, S.; Derkatch, A.; Semaniak, J.; Neau, A.; Al-Khalili, A.; Le Padellec, A.; Vikor, R.; Thomas, R.; Danared, H.; af Ugglas, M.; Larsson, M. *J. Chem. Soc., Faraday Discuss.* **2000**, *115*, 295.

(33) *Average Energy Required to Produce an Ion Pair*, ICRU Report 31; International Commission on Radiation Units and Measurements: Washington, D.C., 1979.